

## Chalcogenides

DOI: 10.1002/ange.200502787

**Acid-Induced Conversions in Open-Framework Semiconductors: From  $[\text{Cd}_4\text{Sn}_3\text{Se}_{13}]^{6-}$  to  $[\text{Cd}_{15}\text{Sn}_{12}\text{Se}_{46}]^{14-}$ , a Remarkable Disassembly/Reassembly Process\*\****Nan Ding and Mercuri G. Kanatzidis\**

The assembly of chalcogenides with 3D open frameworks is of considerable scientific interest because, like the zeolites, they have large free spaces.<sup>[1–3]</sup> Yet due to their greater chemical, compositional, and structural diversity, the chalcogenides present a wider variety and broader scope of properties. These materials can be relevant in molecular recognition,<sup>[2a]</sup> ion conduction,<sup>[3c]</sup> environmental remediation,<sup>[4]</sup> and photocatalysis.<sup>[5]</sup> The chalcogen elements can impart novel photonic or electronic properties that are not found in zeolites.<sup>[3]</sup>

---

[\*] N. Ding, Prof. M. G. Kanatzidis  
Department of Chemistry  
Michigan State University  
East Lansing MI 48842-1793 (USA)  
Fax: (+1) 517-355-1793  
E-mail: kanatzid@cem.msu.edu

[\*\*] Financial support from the National Science Foundation (DMR-0443785 and CHE-0211029 Chemistry Research Group) is gratefully acknowledged.



Supporting information for this article is available on the WWW under <http://www.angewandte.org> or from the author.

However, the ability of zeolites (for example, H-Y, H-ZSM-5<sup>[6]</sup>) to act as solid-acid catalysts is not shared by open-framework chalcogenides, because the chalcogenides are more vulnerable to attack by acid. The 3D open framework of  $K_6Cd_4Sn_3Se_{13}$  contains intersecting tunnels that enable fast ion exchange with alkali-metal cations.<sup>[7]</sup> The observation of efficient ion exchange in  $K_6Cd_4Sn_3Se_{13}$  led to our idea of making proton-exchanged  $H_6Cd_4Sn_3Se_{13}$ , which would contain alkali-metal-free tunnels, through the direct reaction of  $K_6Cd_4Sn_3Se_{13}$  with acid. Our attempt to make  $H_6Cd_4Sn_3Se_{13}$  led to the generation of the new 3D anionic framework  $[Cd_{15}Sn_{12}Se_{46}]^{14-}$ , which shows surprising resistance to acids, as well as excellent ion-exchange properties. Although the number of open-framework chalcogenides has been steadily increasing, reactivity studies on these materials have not been emphasized to date. Herein, we give one of the first reports on the reactivity of these compounds.

After stirring  $K_6Cd_4Sn_3Se_{13}$  in a concentrated aqueous solution of HI (pH 1.1–1.8) for 1 h, the original cube-shaped crystals (Figure 1a) disappeared and new crystals with a

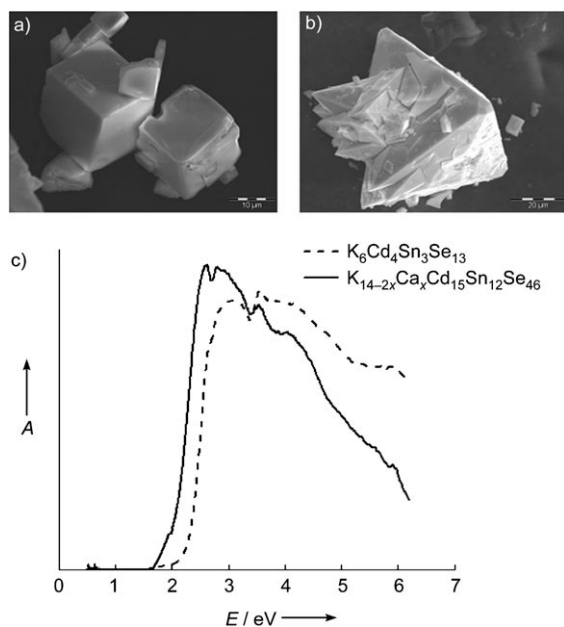


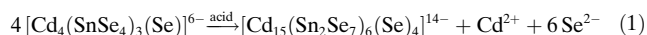
**Figure 1.** a) Scanning electron microscope (SEM) image of the original crystals of  $K_6Cd_4Sn_3Se_{13}$ . b) SEM image of the new crystals of  $K_{14-x}H_xCd_{15}Sn_{12}Se_{46}$ . c) Electronic spectra of  $K_6Cd_4Sn_3Se_{13}$  (dashed line) and  $K_{14-2x}Ca_xCd_{15}Sn_{12}Se_{46}$  (solid line).

tetrahedral morphology (Figure 1b) were formed. Single-crystal X-ray diffraction analysis revealed that the new compound has the formula  $K_{14-x}H_xCd_{15}Sn_{12}Se_{46}$  ( $x \approx 7$ ) and a unit cell that is unrelated to that of  $K_6Cd_4Sn_3Se_{13}$ .<sup>[8]</sup> Furthermore, the new structure is comprised of  $[Sn_2Se_7]^{6-}$  ions, rather than the  $[SnSe_4]^{4-}$  ions found in  $K_6Cd_4Sn_3Se_{13}$ .

Interestingly, the isostructural compounds  $K_{14-2x}M_xCd_{15}Sn_{12}Se_{46}$  ( $M = Ca, Mg; x \approx 1.5, 4$ ) were formed under the hydrothermal conditions used to synthesize the original compound  $K_6Cd_4Sn_3Se_{13}$ ,<sup>[7]</sup> by simply adding  $Ca^{2+}$  or  $Mg^{2+}$  ions. The hydrothermal synthesis of

$K_{14-2x}M_xCd_{15}Sn_{12}Se_{46}$ , in a yield of approximately 70%, is complete within 18–24 h, whereas the formation of  $K_6Cd_4Sn_3Se_{13}$  usually requires 3–4 days.<sup>[9,10]</sup> To obtain an analogue with only  $K^+$  ions, it was necessary to carry out the hydrothermal reaction of the starting materials  $K_2Se$ , Cd, Sn, and Se at a higher temperature.<sup>[11,12]</sup> The greater dissociation rate of water at higher temperatures and pressures generates more  $H^+$  ions, which may help in the formation of the  $[Sn_2Se_7]^{6-}$  ions. The compound  $K_{14-2x}Ca_xCd_{15}Sn_{12}Se_{46}$  is a wide-gap semiconductor with an energy gap of approximately 2.00 eV, which is narrower than that of  $K_6Cd_4Sn_3Se_{13}$  (2.33 eV), Figure 1c.

Although the mechanism behind the transformation of  $K_6Cd_4Sn_3Se_{13}$  to  $K_{14-x}H_xCd_{15}Sn_{12}Se_{46}$  is not clear, the reaction is not topotactic, but involves a dissolution/reassembly process. We describe the process on the basis of the building blocks of the two anionic frameworks  $[Cd_4Sn_3Se_{13}]^{6-}$  and  $[Cd_{15}Sn_{12}Se_{46}]^{14-}$  in Equation (1). In this reaction, either a protogenic acid or a Lewis acid such as an  $M^{2+}$  ion, can be used to condense two of the original  $[SnSe_4]^{4-}$  units into a single  $[Sn_2Se_7]^{6-}$  dimeric unit, with the expulsion of  $Se^{2-}$  ions. In addition, some  $Cd^{2+}$  ions are expelled during the formation of the final structure. Considering that selenides are generally vulnerable to acid attack, one of the most amazing properties of the  $[Cd_{15}Sn_{12}Se_{46}]^{14-}$  framework is its high resistance to acid (up to pH 1.1). This feature may be due to the compact 3D arrangement of the building fragments.



The new compounds crystallize in the noncentrosymmetric space group  $I\bar{4}3d$ . Figure 2a shows a  $[100]$  projection of the  $[Cd_{15}Sn_{12}Se_{46}]^{14-}$  framework in the structure of  $K_{14-2x}Ca_xCd_{15}Sn_{12}Se_{46}$ . Surprisingly, the unique framework is based on dimeric  $[Sn_2Se_7]^{6-}$  units linked by  $Cd^{2+}$  ions. The formula of the framework can be more expressly written as  $[Cd_{15}(Sn_2Se_7)_6(\mu_3-Se)_4]^{14-}$ .

The high structural complexity makes it difficult to define a suitable building block in this extended framework. One possibility is the complex fragment with the formula  $[Cd_{15}(Sn_2Se_7)_6(\mu_3-Se)_4]^{14-}$  shown in Figure 2b. At its center there is a  $\mu_3$ -Se atom (Se5) with a triangular planar geometry. To simplify the description, one third of the building block ( $[Cd_5(Sn_2Se_7)_2(\mu_3-Se)]^{14/3-}$ ) is singled out and shown in Figure 2c. The inset of Figure 2c shows the spatial disposition of the metal atoms in this fragment—two vertex-sharing trigonal bipyramids whose trigonal axes are perpendicular to each other. The five Cd atoms (one Cd1 atom and four Cd2 atoms) in this fragment define the center and four vertices of a tetrahedron, which can be used to represent the whole  $[Cd_5(Sn_2Se_7)_2(\mu_3-Se)]^{14/3-}$  unit. As shown in Figure 2d, one way of viewing the  $[Cd_{15}(Sn_2Se_7)_6(\mu_3-Se)_4]^{14-}$  building block is simply as three such tetrahedra linked through a  $\mu_3$ -Se5 atom.

Two of these large  $[Cd_{15}(Sn_2Se_7)_6(\mu_3-Se)_4]^{14-}$  building blocks connect to form a distorted trigonal prism, shown in polyhedral representations viewed perpendicular and parallel to the trigonal axis of the cage in Figures 3a and 3b, respectively. The height of the cage is approximately 6.3 Å (excluding the van der Waals radii of the Se atoms), and in

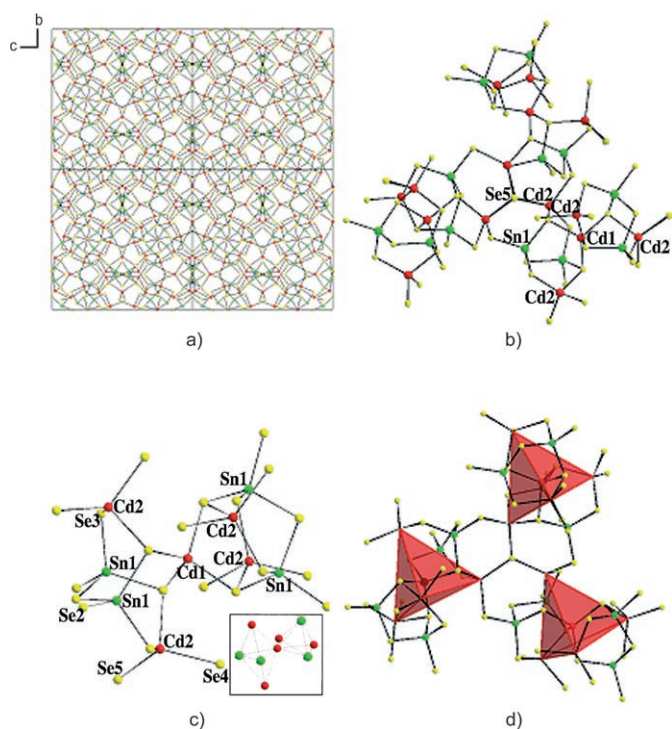


**Figure 2.** a) A [100] projection of the extended  $[\text{Cd}_{15}\text{Sn}_{12}\text{Se}_{46}]^{14-}$  framework, in the structure of  $\text{K}_{14-2x}\text{Ca}_x\text{Cd}_{15}\text{Sn}_{12}\text{Se}_{46}$ . b) The  $[\text{Cd}_{15}(\text{Sn}_2\text{Se}_7)_6(\mu_3\text{-Se})_4]^{14-}$  building block, which is composed of three of the cluster units shown in (c) linked through a  $\mu_3\text{-Se5}$  atom. c) A  $[\text{Cd}_5(\text{Sn}_2\text{Se}_7)_2(\mu_3\text{-Se})_4/3]^{14/3-}$  cluster unit. The inset shows the spatial disposition of the metal atoms. d) A polyhedral representation of the  $[\text{Cd}_{15}(\text{Sn}_2\text{Se}_7)_6(\mu_3\text{-Se})_4]^{14-}$  building block. The red tetrahedra are defined by the five Cd atoms in the cluster unit shown in (c). Cd red, Sn green, Se yellow. Selected bond lengths [Å]: Sn1–Se1 2.530(3), Sn1–Se2 2.547(3), Sn1–Se3 2.500(3), Sn1–Se4 2.492(3), Cd1–Se1 2.632(2), Cd2–Se1 2.688(3), Cd2–Se3 2.625(3), Cd2–Se4 2.652(3), Cd2–Se5 2.6150(17).

$\text{K}_{14}\text{Cd}_{15}\text{Sn}_{12}\text{Se}_{46}$  disordered  $\text{K}^+$  ions occupy approximately half of its space.

In  $\text{K}_{14-2x}\text{M}_x\text{Cd}_{15}\text{Sn}_{12}\text{Se}_{46}$ ,  $\text{M}^{2+}$  ions replace the  $\text{K}^+$  ions in the site near the center of the cage (Figure 3a).<sup>[13]</sup> A view down the [111] direction of the  $[\text{Cd}_{15}\text{Sn}_{12}\text{Se}_{46}]^{14-}$  framework, in which only the cages whose axial directions are parallel to [111] are visible, is shown in Figure 3c. The same pattern is obtained in views down the  $[\bar{1}\bar{1}\bar{1}]$ ,  $[\bar{1}11]$ , and  $[\bar{1}\bar{1}1]$  directions. Therefore, there are cages of four different orientations in the framework, and they are connected by sharing the  $[\text{Cd}_5(\text{Sn}_2\text{Se}_7)_2(\mu_3\text{-Se})_4/3]^{14/3-}$  units. Since the cages are capped by the tetrahedral building blocks, no open channels are readily seen in the unit cell.

The relative size, shape, and interconnection of the open channels in the  $[\text{Cd}_{15}\text{Sn}_{12}\text{Se}_{46}]^{14-}$  framework is revealed by plotting the isosurface lying between the framework atoms and the voids,<sup>[14]</sup> as depicted in Figure 3d along the [111] direction. There are two types of cavities: a) the small spherical voids, which correspond to the small spaces inside the  $\text{Cd}_5\text{Sn}_2$  trigonal bipyramids shown in Figure 2c and have a diameter of only approximately 2.5 Å, and b) the larger trigonal cavities, which lie inside the distorted trigonal prisms shown in Figure 3a and have a diameter of approximately

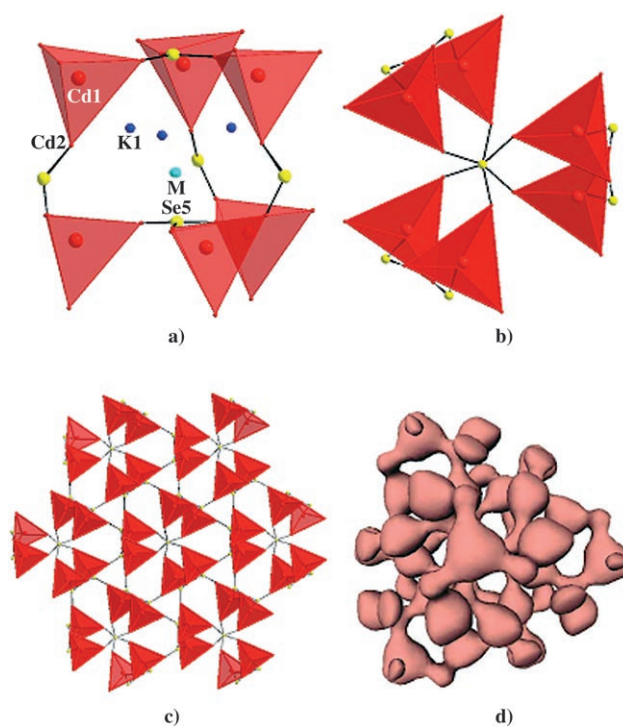


**Figure 3.** a) Polyhedral representation of a single cage, and the  $\text{K}^+$  and  $\text{M}^{2+}$  ions ( $\text{M} = \text{Ca}, \text{Mg}$ ) contained within it, in the structure of  $\text{K}_{14-2x}\text{M}_x\text{Cd}_{15}\text{Sn}_{12}\text{Se}_{46}$ . b) The same cage viewed down its threefold axis. c) Polyhedral representation of the  $[\text{Cd}_{15}\text{Sn}_{12}\text{Se}_{46}]^{14-}$  framework viewed down the [111] direction. The red polyhedra are defined by the five Cd atoms in Figure 2c, and the yellow balls are  $\mu_3\text{-Se5}$  atoms. d) Depiction of the void space in  $[\text{Cd}_{15}\text{Sn}_{12}\text{Se}_{46}]^{14-}$  along the [111] direction. See text for details.

6 Å. These two types of cavities are connected by narrow channels whose width is approximately 2 Å to form a 3D labyrinthine network of cages.

The presence of interconnected cages in the structure enables large ion mobilities and fast ion exchange. Ion-exchange reactions with the ions  $\text{Cs}^+$ ,  $\text{Rb}^+$ ,  $\text{Na}^+$ ,  $\text{Li}^+$ , and  $\text{H}^+$  were performed on  $\text{K}_{14}\text{Cd}_{15}\text{Sn}_{12}\text{Se}_{46}$  at room temperature (Table 1).<sup>[15,16]</sup> The mobility of the  $\text{K}^+$  ions is surprisingly high, despite the relatively small diameter of the tunnels. As also observed for  $\text{K}_6\text{Cd}_4\text{Sn}_3\text{Se}_{13}$ ,<sup>[7]</sup>  $\text{Rb}^+$  ions can replace almost all the  $\text{K}^+$  ions in  $\text{K}_{14}\text{Cd}_{15}\text{Sn}_{12}\text{Se}_{46}$  to form  $\text{Rb}_{14}\text{Cd}_{15}\text{Sn}_{12}\text{Se}_{46}$ . The strongly hydrated  $\text{Li}^+$  ion is a larger entity and gives a lower exchange yield than the  $\text{Cs}^+$ ,  $\text{Rb}^+$ , and  $\text{Na}^+$  ions. In the case of

**Table 1:** Energy dispersive spectroscopy (EDS) analysis of the ion-exchange products.

Exchanged cation	EDS analysis	Exchange yield <sup>[a]</sup> [%]
$\text{Cs}^+$	$\text{K}_{1.44}\text{Cs}_{8.64}\text{Cd}_{15.12}\text{Sn}_{12}\text{Se}_{43.08}$	86
$\text{Rb}^+$	$\text{K}_{0.84}\text{Rb}_{13.92}\text{Cd}_{14.76}\text{Sn}_{12}\text{Se}_{42.36}$	94
$\text{Na}^+$	$\text{K}_{1.56}\text{Na}_{11.40}\text{Cd}_{14.04}\text{Sn}_{12}\text{Se}_{48.0}$	88
$\text{Li}^+$	$\text{K}_{8.88}\text{Cd}_{13.32}\text{Sn}_{12}\text{Se}_{46.08}$	37
$\text{H}^+$	$\text{K}_{4.68}\text{Cd}_{12.48}\text{Sn}_{12}\text{Se}_{43.08}$	67

[a] In the cases of  $\text{Li}^+$  and  $\text{H}^+$  ion exchange, the yield is calculated based on the theoretical formula  $\text{K}_{14}\text{Cd}_{15}\text{Sn}_{12}\text{Se}_{46}$ ; all other yields are calculated based on the amount of cations detected.

H<sup>+</sup> ion exchange, approximately 2/3 of the K<sup>+</sup> ions were exchanged when a concentrated acid solution (pH 1.7) was used. When the pH was 2.3, almost no exchange of K<sup>+</sup> ions was observed.

In a remarkable acid-induced 3D-to-3D transformation at room temperature, K<sub>6</sub>Cd<sub>4</sub>Sn<sub>3</sub>Se<sub>13</sub> was converted into K<sub>14-x</sub>H<sub>x</sub>Cd<sub>15</sub>Sn<sub>12</sub>Se<sub>46</sub>, which adopts a new structure type. The [Cd<sub>15</sub>Sn<sub>12</sub>Se<sub>46</sub>]<sup>14-</sup> framework, which contains a tunnel network of accessible cages of labyrinthine complexity, is highly robust and acid resistant. The new structure type may serve as a suitable model for understanding the structures of amorphous mesostructured chalcogenides,<sup>[17,18]</sup> for example, the mesostructured "Pt-SnSe<sub>4</sub>," which also shows marked resistance to acids and excellent ion-exchange properties.<sup>[19]</sup>

Received: August 5, 2005

Revised: November 22, 2005

Published online: January 20, 2006

**Keywords:** chalcogenides · hydrothermal synthesis · ion-exchange · open-framework structures · semiconductors

- [1] a) S. Dhingra, M. G. Kanatzidis, *Science* **1992**, 258, 1769; b) T. J. McCarthy, T. A. Tanzer, M. G. Kanatzidis, *J. Am. Chem. Soc.* **1995**, 117, 1294; c) J. A. Hanko, M. G. Kanatzidis, *Angew. Chem.* **1998**, 110, 354; *Angew. Chem. Int. Ed.* **1998**, 37, 342; d) A. Enos Axtell III, Y. Park, K. Chondroudis, M. G. Kanatzidis, *J. Am. Chem. Soc.* **1998**, 120, 124; e) M. J. Manos, R. G. Iyer, E. Quarez, J. H. Liao, M. G. Kanatzidis, *Angew. Chem.* **2005**, 117, 3552; *Angew. Chem. Int. Ed.* **2005**, 44, 3618.
- [2] a) H. Li, A. Laine, M. O'Keefe, O. M. Yaghi, *Science* **1999**, 283, 1145; b) H. Li, J. Kim, T. L. Groy, M. O'Keefe, O. M. Yaghi, *J. Am. Chem. Soc.* **2001**, 123, 4867; c) H. Li, J. Kim, M. O'Keefe, O. M. Yaghi, *Angew. Chem.* **2003**, 115, 1817; *Angew. Chem. Int. Ed.* **2003**, 42, 1819.
- [3] a) N. Zheng, X. Bu, P. Feng, *Angew. Chem.* **2004**, 116, 4857; *Angew. Chem. Int. Ed.* **2004**, 43, 4753; b) N. Zheng, X. Bu, P. Feng, *Nature* **2003**, 426, 428; c) X. Bu, N. Zheng, Y. Li, P. Feng, *J. Am. Chem. Soc.* **2003**, 125, 6024; d) N. Zheng, X. Bu, B. Wang, P. Feng, *Science* **2002**, 298, 2366; e) C. Wang, X. Bu, N. Zheng, P. Feng, *J. Am. Chem. Soc.* **2002**, 124, 10268.
- [4] C. L. Cahill, J. B. Parise, *J. Chem. Soc. Dalton Trans.* **2000**, 1475.
- [5] a) N. Zheng, X. Bu, P. Feng, *J. Am. Chem. Soc.* **2005**, 127, 5286; b) N. Zheng, X. Bu, P. Feng, *Chem. Commun.* **2005**, 2805.
- [6] T. Okuhara, *Chem. Rev.* **2002**, 102, 3641.
- [7] N. Ding, D.-Y. Chung, M. G. Kanatzidis, *Chem. Commun.* **2004**, 1170.
- [8] K<sub>14-x</sub>H<sub>x</sub>Cd<sub>15</sub>Sn<sub>12</sub>Se<sub>46</sub> ( $x \approx 7$ ) crystal data: A tetrahedron-shaped crystal with dimensions  $0.065 \times 0.059 \times 0.053 \text{ mm}^3$  was chosen for the single-crystal X-ray diffraction experiment. An empirical absorption correction was applied to the data using SADABS. The structure was solved by direct methods and refined using SHELX-97. K<sub>7.92</sub>H<sub>6.08</sub>Cd<sub>15</sub>Sn<sub>12</sub>Se<sub>46</sub>,  $M_r = 7058.38$ , cubic, space group  $I\bar{4}3d$  (No. 220),  $a = 23.0897(5) \text{ \AA}$ ,  $V = 12309.9(5) \text{ \AA}^3$ ,  $Z = 4$ ,  $\rho_{\text{calcd}} = 3.790 \text{ mg m}^{-3}$ ,  $\mu = 18.763 \text{ mm}^{-1}$ ; index range  $-27 \leq h \leq 27$ ,  $-27 \leq k \leq 27$ ,  $-27 \leq l \leq 27$ ; total reflections 42734, independent reflections 1815, parameters 65,  $R1 = 0.0840$ ,  $wR2 = 0.2085$ ,  $\text{GOF} = 0.950$ . The crystals diffracted X-rays poorly. The K<sup>+</sup> ions are disordered over several sites in the cavity. Energy dispersive spectroscopy (EDS) analysis of the single crystal: K<sub>4.8</sub>Cd<sub>12.0</sub>Sn<sub>12</sub>Se<sub>45.6</sub>. The structure was not deposited with the ICSD because of the poor diffraction quality of the crystals and the availability of the much better refined structures of the isostructural compounds K<sub>14-2x</sub>M<sub>x</sub>Cd<sub>15</sub>Sn<sub>12</sub>Se<sub>46</sub>.
- [9] Synthesis of K<sub>14-2x</sub>M<sub>x</sub>Cd<sub>15</sub>Sn<sub>12</sub>Se<sub>46</sub> (M = Ca, Mg;  $x \approx 1.5, 4$ ): K<sub>2</sub>Se (0.093 g, 0.6 mmol), Cd (0.143 g, 1.3 mmol), Sn (0.120 g, 1.0 mmol), and Se (0.260 g, 3.3 mmol) were combined in an evacuated and flame-sealed fused-silica tube, and melted at 900 °C. The product was loaded into a 9-mm pyrex tube along with CaCl<sub>2</sub> (0.066 g, 0.6 mmol) or MgCl<sub>2</sub>·6H<sub>2</sub>O (0.145 g, 0.7 mmol), and deionized water (0.2 mL). The tube was then evacuated to  $3 \times 10^{-3}$  Torr and flame sealed. The tube was kept at 115 °C for 18–24 h. The products, dark orange tetrahedral or polyhedral crystals, were collected by filtration, and washed with water, ethanol, and diethyl ether. Yield: 70%. The main impurity is K<sub>2</sub>CdSnSe<sub>4</sub> (ca. 30%). The crystals are stable in air for months. The powder X-ray diffraction patterns of K<sub>14-2x</sub>M<sub>x</sub>Cd<sub>15</sub>Sn<sub>12</sub>Se<sub>46</sub> are identical to that of K<sub>14-x</sub>H<sub>x</sub>Cd<sub>15</sub>Sn<sub>12</sub>Se<sub>46</sub>, demonstrating that the compounds are isostructural.
- [10] K<sub>14-2x</sub>Ca<sub>x</sub>Cd<sub>15</sub>Sn<sub>12</sub>Se<sub>46</sub> ( $x \approx 1.5$ ) crystal data: A polyhedron-shaped crystal with dimensions  $0.085 \times 0.102 \times 0.093 \text{ mm}^3$  was chosen for the single-crystal X-ray diffraction experiment. An empirical absorption correction was applied to the data using SADABS. The structure was solved with direct methods and refined using SHELX-97. K<sub>6.6</sub>Ca<sub>0.8</sub>Cd<sub>15</sub>Sn<sub>12</sub>Se<sub>46</sub>,  $M_r = 7031.99$ , cubic,  $I\bar{4}3d$  (No. 220),  $a = 23.2807(4) \text{ \AA}$ ,  $V = 12617.9(4) \text{ \AA}^3$ ,  $Z = 4$ ,  $\rho_{\text{calcd}} = 3.807 \text{ mg m}^{-3}$ ,  $\mu = 18.500 \text{ mm}^{-1}$ ; index range  $-27 \leq h \leq 27$ ,  $-27 \leq k \leq 27$ ,  $-27 \leq l \leq 15$ ; total reflections 30752, independent reflections 1855, parameters 66,  $R1 = 0.0516$ ,  $wR2 = 0.1337$ ,  $\text{GOF} = 1.140$ . The K<sup>+</sup> and Ca<sup>2+</sup> ions are disordered over several sites in the cavity. EDS analysis of the single crystal: K<sub>10.4</sub>Ca<sub>1.3</sub>Cd<sub>14.9</sub>Sn<sub>12</sub>Se<sub>43.7</sub>. Further details of the crystal structure investigation may be obtained from the Fachinformationszentrum Karlsruhe, 76344 Eggenstein-Leopoldshafen, Germany (fax: (+49)7247-808-666; e-mail: crysdata@fiz-karlsruhe.de) on quoting the deposition number CSD-415497.
- [11] Synthesis of K<sub>14</sub>Cd<sub>15</sub>Sn<sub>12</sub>Se<sub>46</sub>: K<sub>2</sub>Se (0.186 g, 1.2 mmol), Cd (0.286 g, 2.6 mmol), Sn (0.240 g, 2.0 mmol), and Se (0.520 g, 6.6 mmol) were combined in an evacuated and flame-sealed fused-silica tube, and melted at 900 °C. The product was loaded into a 13-mm pyrex tube along with deionized water (0.3 mL). The tube was then evacuated to  $3 \times 10^{-3}$  Torr and flame sealed. The tube was kept at 180 °C for 6 days. Dark orange polyhedral crystals were isolated in 61% yield. The impurities are K<sub>2</sub>CdSnSe<sub>4</sub> (ca. 29%), CdSe (ca. 10%), and a small amount of Se.
- [12] K<sub>14</sub>Cd<sub>15</sub>Sn<sub>12</sub>Se<sub>46</sub> crystal data: A polyhedron-shaped crystal with dimensions  $0.115 \times 0.096 \times 0.098 \text{ mm}^3$  was chosen for the single-crystal X-ray diffraction experiment. An empirical absorption correction was applied to the data using SADABS. The structure was solved with direct methods and refined using SHELX-97. K<sub>14</sub>Cd<sub>15</sub>Sn<sub>12</sub>Se<sub>46</sub>,  $M_r = 7989.84$ , cubic,  $I\bar{4}3d$  (No. 220),  $a = 23.090(3) \text{ \AA}$ ,  $V = 12311(3) \text{ \AA}^3$ ,  $Z = 4$ ,  $\rho_{\text{calcd}} = 3.933 \text{ mg m}^{-3}$ ,  $\mu = 19.001 \text{ mm}^{-1}$ ; index range  $-27 \leq h \leq 27$ ,  $-27 \leq k \leq 27$ ,  $-27 \leq l \leq 27$ ; total reflections 73484, independent reflections 1815, parameters 67,  $R1 = 0.0768$ ,  $wR2 = 0.1874$ ,  $\text{GOF} = 1.210$ . The K<sup>+</sup> ions are disordered over several sites in the cavity. EDS analysis of the single crystal: K<sub>12.4</sub>Cd<sub>14.5</sub>Sn<sub>12</sub>Se<sub>44.0</sub>. Further details of the crystal structure investigation may be obtained from the Fachinformationszentrum Karlsruhe, 76344 Eggenstein-Leopoldshafen, Germany (fax: (+49)7247-808-666; e-mail: crysdata@fiz-karlsruhe.de) on quoting the deposition number CSD-415498.
- [13] See Supporting Information for further discussion of the cationic site occupancy.
- [14] T. F. Nagy, S. D. Mahanti, J. L. Dye, *Zeolites* **1997**, 19, 57. See Supporting Information for further explanation of the calculation of the free space.

- [15] A typical ion-exchange reaction with  $H^+$  ions:  $K_{14}Cd_{15}Sn_{12}Se_{46}$  (20 mg) was mixed with an aqueous solution of HI (pH 1.7, 15 mL). The mixture was left at room temperature for 5.5 h without stirring. The product was collected by filtration, and washed with water, ethanol, and diethyl ether. The crystallinity of the sample was confirmed by X-ray powder diffraction before and after the ion exchange. The extent of the ion exchange was assessed with EDS analysis.
- [16] A typical ion-exchange reaction with  $A^+$  ions ( $A = Li, Na, Rb, Cs$ ):  $K_{14}Cd_{15}Sn_{12}Se_{46}$  (40 mg) was mixed with an aqueous solution of  $A^+$  ions (LiI, NaI, RbCl, or  $CsCH_3COO$ ; ca. 20 equiv, 10 mL) at room temperature and stirred for 5 h. The products were collected by filtration, and washed with water, ethanol, and diethyl ether. The crystallinity of the samples was confirmed by X-ray powder diffraction before and after the ion exchange. The extent of the ion exchange was assessed with EDS analysis.
- [17] P. N. Trikalitis, K. K. Rangan, M. G. Kanatzidis, *J. Am. Chem. Soc.* **2002**, *124*, 2604.
- [18] P. N. Trikalitis, K. K. Rangan, T. Bakas, M. G. Kanatzidis, *Nature* **2001**, *410*, 671.
- [19] P. N. Trikalitis, N. Ding, C. Malliakas, S. J. L. Billinge, M. G. Kanatzidis, *J. Am. Chem. Soc.* **2004**, *126*, 15326.